Computational modeling of asphalt pavement resilience to flooding

Xiao Chen
Rutgers University, Piscataway, NJ, 08854, USA

Hao Wang
**Corresponding author, Email: hwang.cee@rutgers.edu*

Rutgers University, Piscataway, NJ, 08854, USA

ABSTRACT: Flooding has multifarious impacts on asphalt pavement performance. This study provides a framework to comprehensively assess the asphalt pavement resilience to flooding by integrated computational modeling, addressing both surface and subsurface aspects. A hydro-mechanical mode was developed to evaluate the hydraulic scouring effect on the fully saturated areas on asphalt surface layer. From subsurface aspect, subsurface saturation profiles during inundation and recovery were first analyzed using a hydrological model. Based on saturation variations, a mechanistic model was developed to quantify the damage caused by subsurface weakening, and the previous hydro-mechanical model was adopted to evaluate the subgrade erosion potential. The proposed methodology provides an effective way to analyze various flooding impact mechanisms on asphalt pavement performance over both short- and long-term.

1 INTRUCTION

Transportation infrastructures, in particular roadway pavements, are increasingly affected by climatic hazards, of which flooding is a major concern. For traditional asphalt pavements, the impact of flooding on pavement performance can be multifarious. Floodwater can infiltrate surface asphalt layers with high air void content (8–10%) (Omar et al. 2020), leaving residual water for up to a week after recession (Guo et al. 2011). Under traffic loading, pore water pressure (PWP) develops, leading to cyclic hydraulic scouring and asphalt performance degradation. For pavement subsurface layers, increased moisture content reduces modulus, diminishing the foundation ability to withstand vehicular stresses and exacerbating structural responses under loading. Additionally, PWP at the subgrade-subbase interface can trigger fines migration (pumping effect), leading to subgrade erosion (Holtz et al. 2008).

Currently, there are research gaps in comprehensively assessing flooding impacts. Firstly, previous studies have focused on pavement performance under fully saturated asphalt layer. In the current practice, dense-graded asphalt pavement is designed to have 4% target air voids that do not allow water to penetrate so that the fully saturation is not the typical condition. Instead, the segregation area, or asphalt patch compacted by shovel or tamper for pothole repair could have high air void contents. Secondly, the current studies on evaluating subsurface weakening effect were limited to pavement response increase right after flooding, which is incomplete without a quantifiable measure of flood-induced damage during the whole recovery period. Thirdly, the subgrade erosion caused by flooding was largely ignored.

2 OBJECTIVE

The objective of this study is to develop computation models for comprehensively evaluating impacts of flooding on surface and subsurface layers of asphalt pavement. The analysis on surface layers is related to short-term and localized failure, and that on subsurface layers is related to long-term pavement deterioration. Figure 1 shows the analysis framework. The suite of computation models includes the following:

1. Evaluate hydraulic scouring effects on surface layer by developing a hydro-mechanical model.
2. Predict subsurface saturation profile during inundation and recovery periods by developing a hydrological model.
3. Quantify subsurface weakening and subgrade erosion using previous hydro-mechanical model.

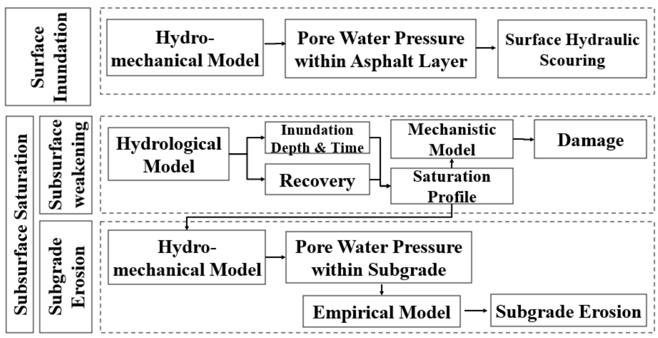

Figure 1. Analysis Framework using Computation Models

3 SURFACE HYDRAULIC SCOURING

3.1 *Development of hydro-mechanical model*

The principle of effective stress was used in this study to characterize the effect of water on mechanical response. On the other hand, Darcy's law was modified to characterize the effect of structure responses on water flow by adding an additional term that reflects the volume change in the voids. For subgrade analysis in following section, Richard's equation was modified to consider unsaturated flow.

The pavement was composed of a 20-cm HMA layer, a 30-cm granular base layer, and subgrade. Three different asphalt patch geometries and various wheel paths were considered, as shown in Figure 2. A single axle with dual tires with speed of 90km/s was simulated, and the tire pressure of 0.7MPa. To consider different properties between asphalt patch and surrounding pavement, different Prony series parameters were used. Detailed model development and material property parameters can be found elsewhere (Chen & Wang 2024a).

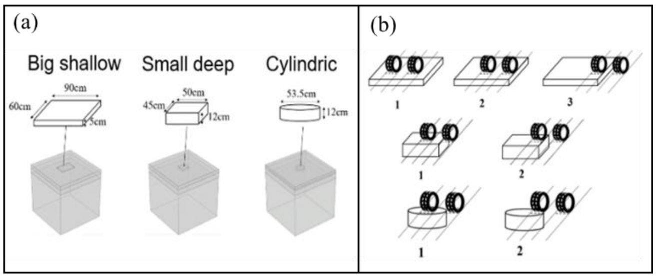

Figure 2. Pothole shapes and wheel paths

3.2 *PWP within asphalt material*

Figure 3(a) compares the maximum PWP within the asphalt patch at 25°C. It can be found that for all three patches, the PWP mainly concentrated underneath the loading area, and the maximum PWP occurred when the vehicle tires just entered the patching area, with a magnitude from 100kPa to 150kPa. Both small-deep and cylindrical patches exhibited larger maximum PWP than the big-shallow patch. Figure 3(b) shows the maximum PWP at the interface, with a magnitude from 100kPa to 200kPa. For cuboid patches, the maximum PWP was at longitudinal interface when vehicle just entered the patch. For cylindrical patch, it occurred at interface when the tire was in the center. When only one vehicle tire travelled through the asphalt patch, the PWP at interface of small-deep patch was the largest, followed by that of cylindrical patch, which is similar as the PWP within the asphalt patch. However, when both tires were loaded on the patch area, the PWP at interface of big-shallow patch became the greatest.

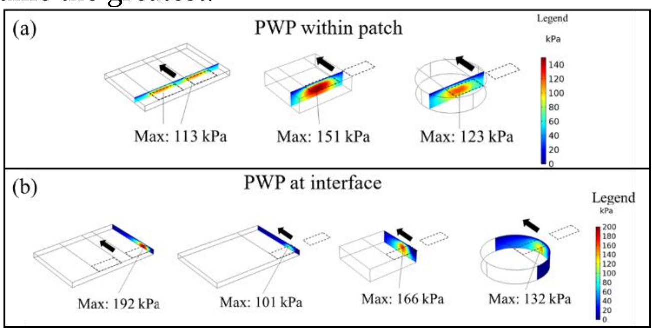

Figure 3 Comparisons of maximum PWP

4 SUBSURFACE SATURATION

4.1 *Development of hydrological model*

Richard's equation, which has been widely used to investigate unsaturated water flow (Dan et al. 2015), was adopted in this study. The Wilson-Penman equation, which is a widely utilized model that integrates different climate factors, was used here to calculate the evaporation rate (Fredlund et al. 2016).

The hydrological analysis was performed for two case studies. One focuses on the flooding event caused by Hurricane Irma in Florida (FL), while the other focuses on the flooding caused by Hurricane Florence in North Carolina (NC). Based on the collected information, the flooded pavement in FL case was composed of a 12.7cm asphalt layer, a 20cm granular aggregate base layer and sand subgrade. For NC case, it is presumed that the structure was the same as that in Florida case, with silt subgrade.

2-D hydrological models were developed. The model geometry is shown in Figure 4. Floodwater head was applied to the unpaved soil surface during inundation. Based on the collected information, the initial groundwater tables (GWT) were set at 0.5 and 1.1 meters below surface in FL and NC cases, respectively. The drainage pipe is placed on the top of subgrade under the shoulder. It aims to remove excessive water from the base layer. During recovery, various weather conditions were collected and utilized for calculating the evaporation rate, which was then subtracted from the precipitation rate to determine the net water influx during the recovery period, which was applied to the exposed soil as a boundary condition. The material properties can be found elsewhere (Zapata 2010). More details on hydrological models can be found elsewhere (Chen & Wang 2024b).

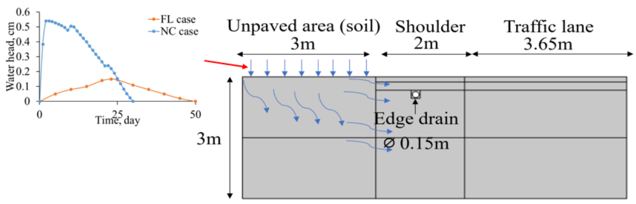

Figure 4. Hydrological model

4.2 *Subsurface moisture variation*

Figure 5 shows the variation of moisture at the surface of exposed soil, middle of base and surface of subgrade. It shows that moisture in both cases illustrates a remarkable daily variation because of the precipitation. This indicates that the moisture at the surface of exposed soil is significantly impact by the environmental factors. The moisture of base and subgrade differs between FL and NC cases because of different initial GWT and soil properties. During the initial phase of recovery period, the unbound materials remained saturated and subsequently began to decrease gradually over time. The recovery time for both cases was around 500 days. Compared with moisture of exposed soil, the effect of precipitation on moisture of pavement unbound material is much less significant. These demonstrates that the moisture within the pavement structure maintains relative stability despite environmental fluctuations.

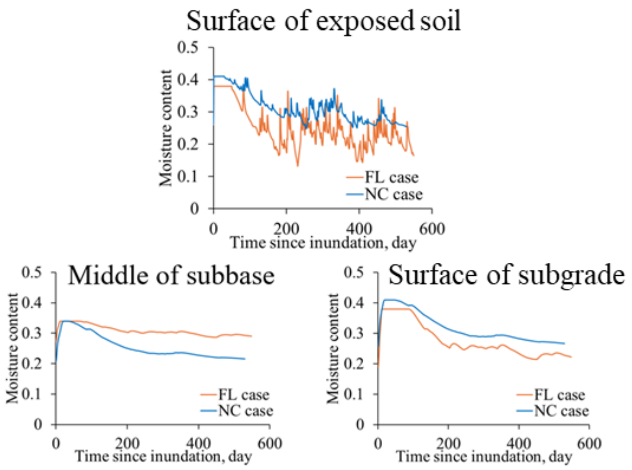

Figure 5. Moisture content variations at different locations

5 SUBSURFACE WEAKENING EFFECT

5.1 *Development of mechanistic model*

According to the pavement structure in FL and NC cases, a 3-D mechanical model was developed to analyze pavement responses under moving loading. For unbound base and subgrade, the moisture-stress-suction dependent modulus model was used in this study. The moisture content distributions obtained from the hydrological model were imported as the initial condition to calculate the non-linear modulus of unbound materials assuming moisture contents do not vary along traffic direction. The detailed model development and material property parameters can be found elsewhere (Chen & Wang 2024c).

Figure 6 shows the critical responses of pavements during recovery. It shows that after full saturation, the maximum increases in tensile strains were 9.5% and 13.2% for FL and NC cases, respectively. In contrast, the increases in compressive strain were much more substantial, rising to 22.8% for the FL case and 37.4% for the NC case. Compared to the increases in tensile strain, the increases in compressive strain are more pronounced. This suggests that the flooded pavements in both cases are more susceptible to subgrade rutting than to fatigue cracking.

5.2 *Damage caused by subsurface weakening*

According to the pavement performance models for asphalt fatigue cracking and subgrade, the pavement responses can be further converted to the allowable loading repetitions to failure. Different axle configurations and load magnitudes in the traffic mix can be converted into the number of equivalent single axle loading (ESAL, 80kN). Therefore, the damage ratio caused by traffic loading for each period after inundation can be calculated. Detailed calculations can be found elsewhere (Chen & Wang 2024d).

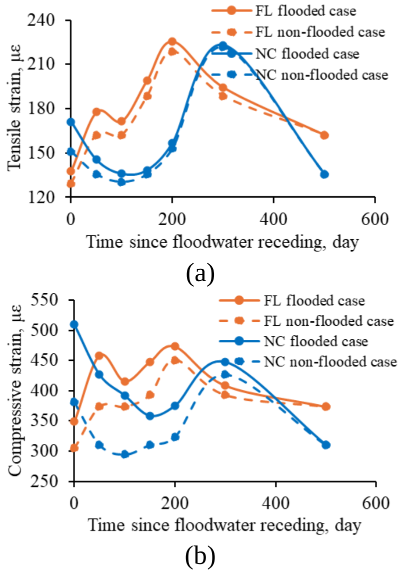

Figure 6. Variations in pavement responses during recovery: (a) Tensile strain at bottom of asphalt layer, (b) Compressive strain at surface of subgrade

Based on the collected information, the daily ESALs was 478 during the recovery period. The daily damage ratios were calculated considering the effect of seasonal temperature variations on asphalt mixtures modulus. It reveals that, compared to the pre-flooding conditions at the end of the recovery period, the difference in damage ratios between flooded and non-flooded cases are substantially higher at the beginning phase of recovery. Figure 7 shows the total damage caused by unbound material modulus reduction during recovery period for FL and NC cases. It shows that the fatigue damage ratio increased by 1.16 times and 1.08 times due to flooding for FL and NC cases, respectively. However, the impact on the subgrade was more significant. Flooding led to subgrade rutting damage rising by 1.38 times for FL case and 1.82 times for NC case.

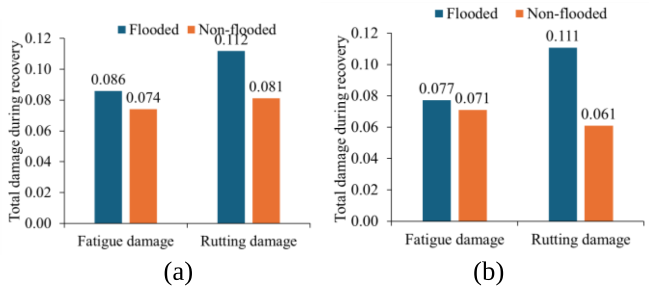

Figure 7. Total pavement damage during recovery period: (a) FL case, (b) NC case

6 SUBGRADE EROSION POTENTIAL

6.1 *PWP within subgrade*

The focus of PWP was at the surface of the subgrade, a location susceptible to erosion due to mass migration to the upper base layer. In the fully saturated state, the PWP under traffic loading reached as high as 10 kPa in the NC case and 8 kPa in the FL case. Based on the findings in the literature (Kermani et al. 2019), this PWP level is high enough to cause mass migration. Following the cessation of traffic loading, the PWP gradually returned to its initial level. Figure 8 depicts the fluctuations in maximum PWP over the recovery period. Although the initial maximum PWP is high, it significantly decreases at around 20 days of recovery. Moreover, the PWP further declines to below zero after about 50 days of recovery in both scenarios. A negative PWP implies that the water within the soil is under tension, a condition that does not cause erosion. Therefore, although the recovery period may extend up to 500 days, the risk of erosion is confined to the first one or two months.

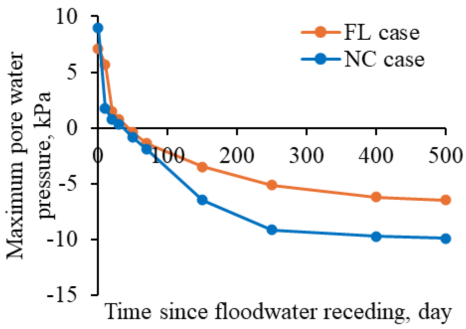

Figure 8. PWP at surface of subgrade during recovery period

6.2 *Subgrade erosion potential*

The mass migration was used in this section to evaluate the subgrade erosion potential due to the generation of PWP. An empirical equation was developed based on laboratory testing results from Kermani et al. (2019). It is important to note that this empirical equation is provided only for illustrative purposes because of limited data. Based on the traffic information during recovery and PWP levels, the total mass migration can be calculated and is shown in Figure 9. The total mass migrations in FL and NC cases are 0.80% and 0.76%, respectively. In the future, it is recommended to conduct detailed analysis on subgrade erosion effects.

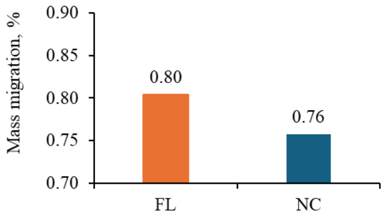

Figure 9. Subgrade erosion in terms of mass migration during recovery

7 CONCLUSIONS

This study developed computation models to comprehensively assess asphalt pavement resilience to flooding from both surface and subsurface aspects. The surface hydraulic scouring effect was characterized by hydro-mechanical model. The subsurface saturation profile was analyzed by hydrological analysis. Based on saturation profiles, a mechanistic model was developed to calculate the critical pavement responses and further quantify the damage caused by subsurface weakening. On the other hand, saturation profiles were also used to evaluate the subgrade erosion potential based on the hydro-mechanical modeling.

The developed computation models allow for comprehensively assessing the impact of flooding on pavement, facilitating the development of resilient pavement designs.

8 REFERENCES

Chen, X., & Wang, H. (2024a). Hydro-mechanical analysis of water-induced pothole patch failure in asphalt pavement. *Construction and Building Materials*, *413*, 134767.

Chen, X. and Wang, H. (2024b). Impact of Sea Level Rise Induced Hazards on Airfield Pavement Performance: A Simulation Study, *Transportation Research Record* (published online)

Chen, X., & Wang, H. (2024c). Evaluation of Pavement Resilience to Flooding with Inverted Pavement Structure. *Road Materials and Pavement Design*.

Chen, X., & Wang, H. (2024d). Post-flooding Asphalt Pavement Condition Assessment for Roadway Operation Strategy. *Journal of Transportation Engineering, Part B: Pavements*, *150*(1), 04023035.

Dan, H. C., He, L. H., Zhao, L. H., & Chen, J. Q. (2015). Coupled hydro-mechanical response of saturated asphalt pavement under moving traffic load. *International Journal of Pavement Engineering*, *16*(2), 125-143.

Fredlund, M. D., Tran, D., & Fredlund, D. G. (2016). Methodologies for the calculation of actual evaporation in geotechnical engineering. *International journal of geomechanics*, *16*(6), D4016014.

Guo, X. D., Cao, J., & Fang, X. Y. (2011). Study of water stability of asphalt mixture based on residual water. *Applied Mechanics and Materials*, *71*, 1791-1794.

Holtz RD, Christopher BR, Berg RR (2008) Geosynthetic design & construction guidelines: reference manual. National Highway Institute, Washington 22.

Kermani, B. et al. (2019). Measuring the migration of subgrade fine particles into subbase using scaled accelerated flexible pavement testing–a laboratory study. *Road Materials and Pavement Design*, *20*(1), 36-57.

Omar, H. A., Yusoff, N. I. M., Mubaraki, M., & Ceylan, H. (2020). Effects of moisture damage on asphalt mixtures. *Journal of Traffic and Transportation Engineering (English Edition)*, *7*(5), 600-628.

Zapata, C. E. (2010). *A national database of subgrade soil-water characteristic curves and selected soil properties for use with the MEPDG*, NCHRP Project 9-23A.